[CANCER RESEARCH 60, 2018–2024, April 1, 2000]

Detection of Hypoxia in Human Squamous Cell Carcinoma by EF5 Binding[1]

Sydney M. Evans,[2] Stephen Hahn, Deirdre R. Pook, W. Timothy Jenkins, Ara A. Chalian, Paul Zhang, Craig Stevens, Randall Weber, Gregory Weinstein, Ivor Benjamin, Natasha Mirza, Mark Morgan, Steven Rubin, W. Gillies McKenna, Edith M. Lord, and Cameron J. Koch

Schools of Veterinary Medicine [S. M. E., D. R. P.] and Medicine [S. H., A. A. C., W. T. J., P. Z., W. G. M., C. J. K., I. B., G. W., N. M., M. M., S. R., R. W.], University of Pennsylvania, Philadelphia, Pennsylvania 19104; The University of Texas M. D. Anderson Cancer Center, Houston, Texas 77030 [C. S.]; and the University of Rochester Cancer Center, Rochester, New York 14642 [E. M. L.]

ABSTRACT

Localization and quantitation of 2-nitroimidazole drug binding in low pO_2 tumors is a technique that can allow the assessment of hypoxia as a predictive assay. EF5 [2-(2-nitro-1*H*-imidazol-1-yl)-*N*-(2,2,3,3,3-pentafluoropropyl) acetamide] is such a drug, and it has been shown to be predictive of radiation response in rodent tumors. Using fluorescence immunohistochemical techniques, we provide data on the presence, distribution, and levels of EF5 binding as a surrogate for hypoxia in human head and neck and uterine cervix squamous cell cancers (SCCs). Six patients with SCC were studied. Four patients had head and neck tumors, and two had uterine cervix cancers. The incubation of fresh tissue cubes in EF3 under hypoxic conditions ("reference binding") demonstrated that all tumors were capable of binding drug, and that this binding varied by a factor of 2.9-fold (174.5–516.1) on an absolute fluorescence scale. In the five patients treated at the lowest drug doses (9 mg/kg), *in situ* binding was quantitatable. For all six patients, the maximum rate of *in situ* binding varied by a factor of 6.7 between the lowest and highest binding tumor (24.8–160.3) on an absolute fluorescence scale. In tumors with high binding regions, intratumoral heterogeneity was large, extending from minimal fluorescence (<1%) up to 88.6% of reference binding. In tumors with minimal binding, there was little intratumoral heterogeneity. These studies demonstrate substantial heterogeneity of *in situ* binding between and within individual squamous cell tumors.

INTRODUCTION

The initial observation that hypoxia was prognostically important in human cancer therapy came from studies in head and neck SCC[3] and uterine cervix SCC. As early as 1964, Kolstad (1) demonstrated that hypoxic foci were present in human uterine cervix cancer. He also showed that tumor pO_2 could be increased by inhalation of pure oxygen. In the mid-1970s, uterine cervix cancer patients with hemoglobin levels <12 g% during radiation therapy (compared with those >12 g%) were found to have a significantly higher pelvic recurrence rate and lower cure rate (2, 3). Similar findings were reported in patients with head and neck cancers (4). The first evidence of the presence and clinical importance of hypoxia in SCC was presented by Gatenby *et al.* (5). Using polarographic needle electrodes, a relationship was demonstrated between the pO_2 in fixed lymph node metastases from head and neck carcinomas and response to radiation therapy. More recently, Eppendorf needle electrode data have been published from multiple institutions demonstrating a correlation between treatment outcome and initial pO_2 in SCC of the head and neck and uterine cervix (6–10). Of particular interest is that in uterine cervix cancer patients, this correlation was not limited to those treated with radiation therapy; recurrence after surgical resection was also correlated to initial tumor pO_2, suggesting that the presence of hypoxia infers a more aggressive clinical phenotype (6, 7).

In addition to polarographic needle electrodes, there currently are two other clinically relevant methods for oxygen measurement: the Comet assay (11) and 2-nitroimidazole binding assays (12–15). The former method measures DNA damage in single cells obtained by fine needle aspirate immediately after an oxygen-sensitive damaging process. The technique was developed for use after a single, relatively large dose of ionizing radiation but has been modified to measure steady-state damage during hypoxia-sensitive chemotherapy (16). 2-Nitroimidazole binding assays provide hypoxia measurements to virtually any degree of spatial resolution and with a multiplicity of detection techniques (17–22). One strength of the nitroimidazole binding technique is that a signal for dead cells is not generated because these cells do not metabolize the drug. The binding techniques also have maximum sensitivity at low pO_2, thus providing a positive signal in the absence of oxygen. Raleigh *et al.* (23) have published examples of *in situ* binding of the 2-nitroimidazole pimonidazole in patients with uterine cervix SCC. Herein, we report the use of EF5 in patients with head and neck SCCs and uterine cervix SCCs. In addition to demonstrating the variety of binding patterns in human SCC cancers, we present quantitative data allowing ranking of the level of binding in individual tumors based upon the highest EF5 binding region in each tissue sampled. Our ability to make these evaluations is based upon detailed calibrations of tissues incubated *in vitro*, under low oxygen partial pressures, with EF3 ("reference binding"), an analogue of EF5. We hypothesize that the tumors with highest level of *in situ* binding relative to their *in vitro* reference binding are the most hypoxic.

MATERIALS AND METHODS

Human Subjects. In February 1998, EF5 was granted investigational new drug status for use in human cancer patients by the Food and Drug Administration, and the Phase I/II protocol was approved by the University of Pennsylvania Institutional Review Board. Written informed consent was obtained from all patients entered. Eligible patients were those undergoing incisional or excisional tumor biopsies for other medical indications. Patients of all ethnic and gender groups were included. Exclusion criteria emphasized a history of grade III or IV peripheral neuropathy as defined by the Cancer Theraputics Evaluation Program/Division of Cancer Therapeutics and Evaluation because neurotoxicity has been a problem in the studies of 2-nitroimidazole compounds used in high, multiple doses as hypoxic cell sensitizers (24). Pregnant patients, patients <18 years of age, and those that were HIV positive were excluded.

Drug Administration and Toxicity. EF5 was supplied by the National Cancer Institute, Division of Cancer Treatment in 100-ml vials containing 3 mg/ml EF5 in 5% dextrose in water and 2.5% alcohol. EF5 was administered i.v. via a peripheral i.v. catheter at a rate no greater than 350 ml/h. The i.v. infusion was over 1–2 h with time of administration determined by the dose of EF5 being studied. Acute toxicity was assessed using NCI, Division of Cancer Treatment Common Toxicity Criteria. Patients were examined for signs and symptoms of toxicity at approximately 1, 6, and 48 h and 28 days after drug

Received 8/17/99; accepted 2/1/00.

The costs of publication of this article were defrayed in part by the payment of page charges. This article must therefore be hereby marked *advertisement* in accordance with 18 U.S.C. Section 1734 solely to indicate this fact.

[1] Supported by Grant RO1 CA75285 (to S. M. E.).

[2] To whom requests for reprints should be addressed, at University of Pennsylvania, School of Medicine, Division of Oncology Research, 195 John Morgan Building, Philadelphia, PA 19104. Phone: (215) 898-0074; Fax: (215) 898-0090; E-mail: sydevans@vet.upenn.edu.

[3] The abbreviations used are: SCC, squamous cell carcinoma; EF5, 2-(2-nitro-1*H*-imidazol-1-yl)-*N*-(2,2,3,3,3-pentafluoropropyl) acetamide; EF3, 2-(2-nitro-1*H*-imidazol-1-yl)-*N*-(3,3,3-trifluoropropyl) acetamide; NCI, National Cancer Institute; HPF, high power field.

Table 1 *Patient signalment and EF5 binding levels*

Patient no.	Age/sex/race[a]	EF5 dose (mg/kg)	Site/histology	Stage[b]	Pre-operative hemoglobin[c] (mg/dl)	Notes regarding tumor obtained at surgery	% reference binding
1	54/F/AA	9	SCC/Cervix	$T_{1b}N_0M_0$	12.3		14.8
3	35/F/AA	9	SCC/Cervix	$T_{2b}N_0M_0$	12.3		6.9
4	55/F/AA	9	SCC/H&N[d] (alveolar ridge)	$T_4N_xM_0$	8.2	Tumor invaded adjacent tissues and lymph nodes	88.6
5	69/M/C	9	SCC/H&N (tonsil)	$T_3N_2M_0$	12.7	EF5 binding in invading lymph node	32.5
6	52/M/AA	9	SCC/H&N (tonsil)	$T_3N_0M_0$	10.1		34.5
7	52/F/AA	12	SCC/H&N (retromolar triangle)	$T_4N_1M_0$	11.0	EF5 binding in invading lymph node	16.5

[a] AA, African American; C, Caucasian.
[b] T, tumor; N, node; M, metastasis.
[c] Normal range: females, 11.8–15.5 g/dl; males, 13.5–17.5 g/dl.
[d] H&N, head and neck cancer.

infusion. At ~28 days after drug infusion, blood chemistries and blood counts were obtained. Evaluation of EF5 in blood and urine samples was performed by high-performance liquid chromatography after dilution with equal volumes of trichloroacetic acid. After centrifugation to remove precipitates, analyses were performed on the supernatants.

Tissue Acquisition. Approximately 48 h (range, 40–55) after completion of drug administration, the tumor was either biopsied or resected. Preceding extensive manipulation, sterile tumor tissue was obtained and placed in iced EXCELL 610 media (JRH Biosciences, Leneka, Kansas) with 15% FCS. These tissues were immediately returned to the laboratory where they were processed to obtain cells for culture and tissues to determine reference EF3 binding (see below). Any extra sterile tissues were placed on moist filter paper, coated with a thin layer of Tissue Tek (OCT compound; Sakura Finetek USA, Inc., Torrence, CA), and frozen on dry ice. To avoid tissue desiccation, samples were placed in airtight containers with chips of ice and held at −80°C prior to analysis of *in situ* EF5 binding (see below).

At the completion of surgery, the tumor specimen was taken to pathology where additional tumor and, if possible, normal adjacent tissues were obtained. These tissues were frozen, as above, until they were probed for EF5 binding.

Determination of Tissue Reference Binding. The purpose of these studies was to determine the maximum binding rate of the tissue *in vitro* using EF3 and low (0.2%) oxygen concentrations. EF3 is a 2-nitroimidazole similar to EF5 with only three fluorine atoms on the side chain. EF3, rather than EF5, was used for determination of reference binding rate in tumor tissue cubes because adducts of the two drugs can be distinguished by specific monoclonal antibodies (for EF3, ELK5-A8; and for EF5, ELK3-51). If EF5 were used for the reference studies, it was considered possible that the *in vitro* binding could be artifactually augmented by preexisting high binding from the *in situ* exposure. The alternative of obtaining an additional biopsy prior to EF5 administration was not possible nor considered practical. The ELK5-A8 antibodies developed against EF3 are only weakly interactive with EF5 adducts.[4] Thus, by using EF3 *in vitro*, possible interference from the *in situ* EF5 exposure was minimized.

To obtain cubes, tissues were sliced at 1.5-mm thickness with a tissue slicer (Thomas-Stadie Riggs Tissue Slicer; Thomas Scientific, Swedesboro, NJ) or crossed #10 and #11 scalpels. Cubes were then diced from the tissue slices. Four or five cubes were placed into each of two vials. Control tissue cubes were stirred at 37°C in medium without EF3. Reference tissue cubes were incubated for 3 h with 200 μM EF3 (the drug exposure used for the cubes was comparable with the *in situ* situation, 590 μM·h) and a gas phase containing 0.2% oxygen. The non-zero oxygen concentration allows nonmaximal EF3 binding at the surface of the cube with respiration-induced severe hypoxia and maximal EF3 binding below the surface. Thus, regions of maximal binding can be analyzed several cell layers from the cube surface, where there is less chance of tissue-sectioning artifacts. After a 3-h incubation at 37°C (total drug exposure 600 μM·h), the samples were frozen on dry ice (as above) until sections could be collected and stained with ELK-A8 antibodies (see below).

Immunohistochemical Staining of Tissues for EF5 Binding: Photography and Analysis of Binding. Frozen tissues from *in situ* exposure to EF5 were brought to −20°C one-half h before sectioning. Sections were made at 10 or 14 μm, fixed, blocked, and stained with ELK3–51 antibody conjugated with Cy3 dye (75 μg/ml), as described previously (25). Two sections were treated without antibody ("no stain") to assess endogenous tissue fluorescence, usually negligible. Other adjacent sections were stained with 75 μg/ml antibody admixed with 0.5 mM EF5 ("competed stain"). This allows for the assessment of nonspecific binding of the antibody because specific binding is overwhelmed by the free drug. The competed stain sections were rinsed with buffer containing 0.25 mM EF5. The technique for immunohistochemistry of EF3 adducts in tissue cube studies was identical to that for EF5 (14) with the exception that ELK5-A8 antibody was used. The competed stain condition for ELK5-A8 antibody contained 1.0 mM EF3 for the antibody and 0.5 mM EF3 for the rinse.

Epifluorescence measurements were made using a Nikon LabPhot microscope with 100-W high pressure mercury arc lamp. Filter cubes were optimized for wavelengths of interest (Omega Optical, Brattleboro, Vermont). A cooled (−25°C) CCD digital camera (Photometrics "Quantix," KF1400; grade I defects) was attached to the microscope via a Diagnostic Instruments HRP060 C-mount adapter. Residual infrared light from the filter cubes was eliminated by two serial XF86 filters (Omega Optical) at the base of the C-mount and an additional infrared filter at the output of the lamp. The manual stage of the microscope was replaced by a Ludl Electronic Products 99S000 automatic stage with 0.1-μm step size. The camera and stage were controlled by a Macintosh 9600 Power PC computer. Software was Scanalytics "IP Lab," a general purpose image analysis program with modular support of the hardware components. This instrumentation allows general purpose control programs to be written. Manual or semiautomatic scanning of the section, setting of camera exposure and focus, and automatic collection of images over a defined area with known positional coordinates can be accomplished. Known positional coordinates allow reimaging of the same portion of a section for reference or after additional staining.

During photography, tissue sections were covered by a hemocytometer coverslip recessed from the section by strips of mylar tape, and the enclosed space was filled with 1% paraformaldehyde in PBS. This provides a uniform optical path and prevents tissue desiccation, which can change the apparent levels of staining.

For each patient, at least two tumor regions and two levels within each region (separated by at least 0.5 mm) were examined for regions of *in situ* EF5 binding. The regions were imaged using a ×10 microscope objective (field size set electronically at 1.05 × 0.7 mm^2), and typically 3 × 3 contiguous fields were examined for each section. To improve camera sensitivity while still providing multiple pixels/cell, each image field consisted of 600 × 400 pixels, each of which was a 2 × 2 bin of the actual camera chip pixels, with 12-bit gray scale resolution.

Immunohistochemical Staining for CD31/PECAM. Some tissue sections were stained for both CD31 and EF5 to determine the spatial relationship between hypoxia and blood vessel distribution. Primary labeled antibodies against CD31 are not available; therefore, we developed a protocol allowing primary staining by a mouse monoclonal to human CD31, followed by labeled secondary antibody (rat antimouse). Sections were blocked with PBS containing 1.5% albumin and 0.3% Tween 20 ("antibody carrier") supplemented by 20% skim milk and 5% rat serum. After rinsing, endogenous peroxidase activity was eliminated by treatment with 3% hydrogen peroxide for 10 min at room temperature. Primary antibody (mouse antihuman CD31; PharMingen 30881A) diluted 1+99 with antibody carrier was added for 1.5 h at room temperature. After rinsing, secondary antibody, also diluted 1+99 (Jackson Labs rat antimouse, peroxidase linked) was added for 45 min. After further

[4] E. M. Lord and C. J. Koch, unpublished information, 1995.

Table 2 *EF5 and EF3 binding values*

Patient no.	Highest EF5 *in situ* binding	Competed stain	No stain	Reference binding	% reference binding	Tumor infiltrating lymph node	Normal tissue *in situ* binding
1	53.6	7.2	10.3	362.7 (est[a])	14.8		7.8, endometrium
3	24.8	5.9	3.6	359.8	6.9		
4	154.6	7.1	10.2	174.5	88.6		
5	97.0	3.2	10.5	298.8	32.5	276	
6	160.3	4.0	11.0	454.1	32.5		15.7 muscle
7	133.4	5.7	13.8	516.1	16.5	135.0	13.7 normal lymph node

[a] Estimated based on average reference binding for patients 3–7.

rinsing, substrate (typically amino-ethyl-carbazole, 0.7 mg/ml in 100 mM acetate buffer, pH 5.5, with 0.03% hydrogen peroxide) was added until sufficient development of color was achieved. The peroxidase stained section was then blocked and stained by anti-EF5 antibodies as described above.

Quantitation and Analysis of EF5 Binding. To quantitatively compare *in situ* EF5 binding with reference binding, an absolute fluorescence scale was required. Although the camera sensitivity is expected to be constant, variations in mercury arc lamp output over a typical lamp lifetime can amount to a factor of 3–4. Day-to-day variations are much smaller but can exceed 100%. Different microscopes may have substantially different outputs, even with the same lamp type and power, depending on the optics, filter bandwidths, attenuation, and others. Finally, the numerical aperture and power of the objectives can vary by large factors. To account for these variations, the fluorescence of a reference thickness of Cy3 dye was determined at the beginning and end of every imaging procedure. The dye standard consisted of Cy3 dye in PBS with 1% paraformaldehyde injected into a standard hemocytometer (thickness of the dye layer, 100 μm). The absorbance of the dye was 1.25 at 549 nm. When stored in the dark at 4°C, the Cy3 dye is stable indefinitely in this solution.[5] The dye was imaged (focusing on the gridlines of the hemocytometer), and the exposure time and average pixel intensity were noted. This fluorescence value was assigned a value of 1000. Most tissues examined had maximal fluorescence less than the dye standard. The absolute fluorescence of any sectional region of interest was obtained by determining actual pixel intensity, dividing by the pixel intensity of the standard, and then multiplying by 1000 times the ratio of exposure times for dye standard and region of interest.

Multiple fields representative of the entire *in situ*-exposed tissue section were imaged. In this preliminary assessment of *in situ* tissue binding, we have considered the average pixel intensity in the region of brightest binding as a representation of the most hypoxic cells. The averages represent the means of the entire region enclosing the brightest cells. Although the eye tends to focus on the brightest spots, the difference in intensity between these and nearby cells is only about 20–40%, and the brightest pixels do not significantly affect the reported averages. Rather, they represent a very small asymmetry of the histogram of overall pixel intensities. These histograms appear to be normally distributed. The tissue cube sections were scanned for the section(s), with maximal binding as the determinant of reference binding.

Light Microscopic Evaluations. Slides stained for EF5 binding were dried and counterstained with H&E and evaluated by a pathologist (P. Z.) to assess the presence of tumor (or normal) tissue. Detailed evaluations of paraffin-embedded tumor specimens (from the primary resection specimen) were performed, and the following histological characteristics were evaluated: differentiation, amount of keratinization, amount and type of host reaction (WBC infiltrate), amount of necrosis, and stromal reaction (desmoplasia). In addition, 10 high power fields were evaluated for the number of mitoses.

Eppendorf Measurements. Tumor oxygenation was measured in anesthetized patients using a polarographic needle electrode (pO_2 Histograph; Eppendorf-Netherler-Hinz, GmbH, Hamburg, Germany). In patients where it was medically appropriate to decrease inhaled oxygen concentration to physiological levels, this was done. In all patients, inhaled oxygen concentration was noted at the time of pO_2 probe placement. All measurements were performed under direct tumor visualization, and two to four separate locations were sampled. Track length was adjusted to the tumor size, and step size was 0.4 mm.

[5] C. J. Koch, unpublished information.

RESULTS

Patients, Drug Administration, and Toxicity. Between March 1998 and February 1999, 12 patients signed informed consent documents and participated in the trial. Six of these patients had SCC tumors; two were from the uterine cervix, and four were from the head and neck (Table 1). The remaining six patients had soft tissue sarcomas and will be reported separately. The four patients with head and neck SCCs had low hemoglobin values (Table 1).

Five patients received 9 mg/kg EF5 and one patient received 12 mg/kg EF5 over 1–2 h through an indwelling catheter (Table 1). There were no clinical or biochemical, acute or late (28 days) toxicities reported. Plasma half-life of EF5 was 13 $\pm$ 1 h (data not shown).[6]

Reference EF3 Binding. In preliminary experiments, using rodent tumor tissue cubes with high cellularity and minimal stroma and necrosis, 1% oxygen in the gas phase was determined to be optimal for incubation of the tissue cubes. This was the oxygen content used for patient 1, but because of the high proportion of stromal tissue and tumor necrosis, respiration-induced maximal hypoxia was likely not achieved. For all subsequent patients, the pO_2 for the cube incubations was decreased to 0.2%. Thus, for patient 1, the mean value of the reference binding for the other five patients was assumed (Table 2). The brightest binding cells within the cube were usually within 3–10 cell layers from the surface as a result of metabolism-induced depletion of oxygen at this tissue depth (Fig. 1). In about one-third of the patients, cubes show quite uniform binding over larger regions rather than the patchy heterogeneous binding shown in Fig. 1. There are a number of possible reasons for this heterogeneity: (*a*) tissue damage that occurs when the tumor tissue is cut into such tiny pieces; (*b*) a lack of uniform surface-section distance resulting from the isolation and treatment of these very small tissue pieces; (*c*) small variations in section thickness; and (*d*) there indeed could be variations in oxygenation on a cell-cell basis at very low oxygen levels because the K_m for inhibition of EF5/EF3 binding is of the order of 0.1% oxygen (26). The maximum fluorescence of the cube sections was determined and found to be quite similar from patient to patient, with a range of 327–905 (Table 2).

***In Situ* Binding.** Substantial heterogeneity in patterns and absolute levels of binding were seen in these six patients. Even at the lowest doses of drug administered (9 mg/kg), the resulting fluorescence signal allowed contrast of *in situ* binding to be observed (Figs. 2 and 3). Intratumoral heterogeneity of binding increased with maximal binding because regions with similar values of minimal binding (2–20) were observed in all tumors. The maximal *in situ* binding was found to be 88.6% of reference binding for the same tissue (Fig. 3). The maximal *in situ* binding varied by a factor of 6.7 between the most and least avidly binding tumors (Table 2). In two of the six tumors, the regions of maximal *in situ* binding were adjacent to regions of macroscopic or microscopic (Fig. 3) necrosis. Maximal *in*

[6] C. J. Koch. Pharmacokinetics of the 2-nitroimidazole EFS in human patients: implications for hypoxic measurements *in vivo*, manuscript in preparation.

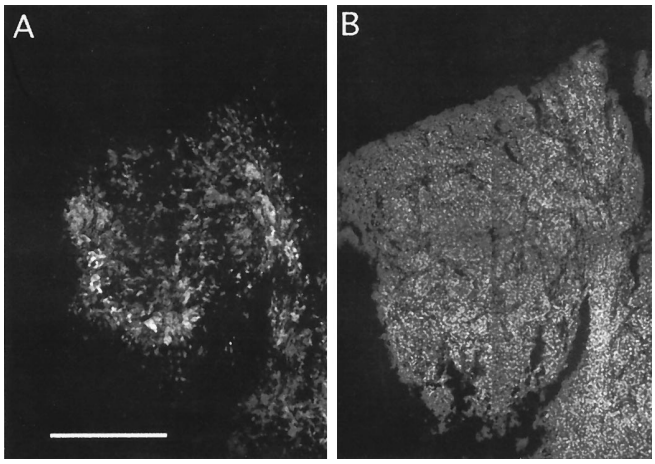

Fig. 1. *A*, photomicrographs of a section from SCC tumor tissue cube (patient 5), incubated *in vitro* in 0.2% oxygen and 600 μM h EF3, for determination of reference binding. Frozen sections were stained with ELK5-A8, and the tissue section of maximal binding was imaged. *B*, the same section as *A* counterstained with Hoescht 33342 to label DNA-containing nuclei in the tissue section. The non-zero oxygen concentration in the suspension allows nonmaximal EF3 binding at the surface of the cube to a depth of ~200 μm from the surface. As a result of respiration-induced severe hypoxia, maximal EF3 binding is seen at depths into the cube greater than ~200 μm. Thus, regions of maximal binding can be analyzed several cell layers from the cube surface, where there is less chance of tissue-sectioning artifacts. *Bar*, 500 μm.

situ binding was associated with keratinized cells in two head and neck tumors (patients 4 and 6).

The regions of maximum fluorescence in the uterine cervix cancer patients comprised similar low values, 14.8% and 6.9% of reference binding (Fig. 2; Table 2). Despite this similarity in maximal fluorescence, the histological appearance of these two tumors differed substantially. The tumor in patient 1 had a corded appearance (Fig. 2, *A* and *B*), whereas the tumor in patient 3 had no obvious organizational pattern (Fig. 2, *C* and *D*). The light microscopic evaluation of these two tumors was also markedly different (Table 3). The tumor in patient 3 was less differentiated, had less necrosis (<10% *versus* 60% in patient 1), and there were many more mitoses (80/10 HPF) compared with patient 1 (40–50/10 HPF). In the corded uterine cervix tumor (Fig. 2), CD31-stained blood vessels were seen at the periphery of the tumor cord. For a radial distance of ~200 μm, there are viable tumor cells that bound little EF5. At greater distance, EF5 binding increases for several cell layers, although only to 15% of reference binding. Centrally, adjacent to these cells, a region of macroscopic necrosis is present.

Intertumoral heterogeneity in binding patterns and levels was present in the patients with head and neck cancer (Fig. 3; Table 2). Regions of *in situ* EF5 binding varied from very high (88.6% of reference binding; patient 4) to moderate (16.5% of maximal, patient 7; Table 2). High EF5 binding adjacent to regions of necrosis was the dominant feature in patient 5. In patients 4 and 6, binding was dominantly in cells in areas of squamous differentiation/keratinization. The head and neck tumor with the most macroscopic necrosis (patient 7) was found to contain only a few scattered regions of bright binding.

Patients 5 and 7 had enlarged lymph nodes on physical examination, and specimens of these tissues were obtained at surgery. On histological examination, both lymph nodes were partially replaced by

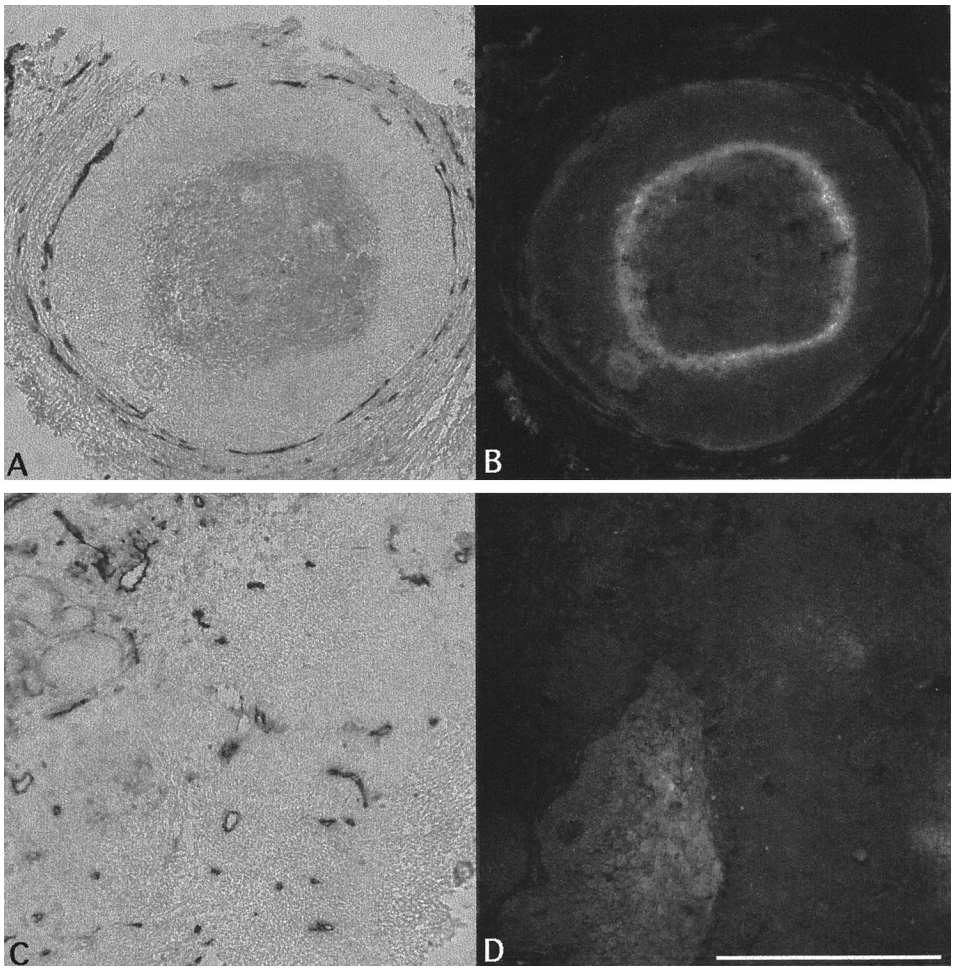

Fig. 2. Photomicrographs showing vessels and hypoxia distribution in two human uterine cervix tumors. *Bar*, 500 μm. The peroxidase-based anti-CD31-stained vessels is indicated by the very densely stained areas. Intermediate levels of gray (*e.g.*, central necrotic portion of the cord in *A*) simply represent contrast in the section. *A* and *B*, the pattern of EF5 binding in this corded cervical SCC (patient 1) is compared with the same region stained for the presence of vasculature (PECAM/CD31). The diameter of the cord of tumor is ~850 μm with vasculature at the periphery. For a radial distance of 125–200 μm from the vessels, there are viable tumor cells that bind little EF5. At greater distances, EF5 binding increases for several cell layers, representing hypoxic, viable cells. Centrally, adjacent to these hypoxic cells, macroscopic necrosis is present. The absolute level of fluorescence in the binding region is relatively low (98.1) yet necrosis occurs. Non-oxygen-related causes of cell death must therefore be considered. *C* and *D*, photomicrographs of region of maximal *in situ* EF5 binding for a noncorded uterine cervix cancer (patient 3) compared with CD31/PECAM stain (performed on an adjacent section). Many vessels are seen, often in close approximation to each other, supporting the relatively low level of binding in this region (fluorescence, 28.1).

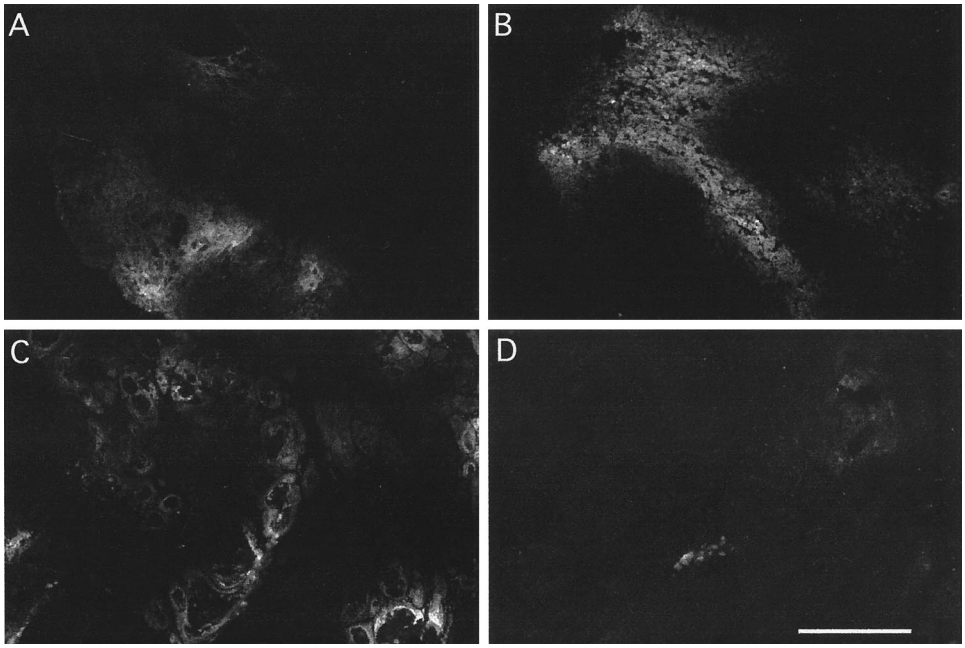

Fig. 3. Photomicrographs comparing patterns of EF5 binding in four head and neck SCCs. Image intensity has been modified to demonstrate distribution of binding. For absolute fluorescence in each section, see Table 2. *Bar*, 500 μm. *A*, patient 4. Bright *in situ* EF5 binding is seen primarily in keratinized cells. *B*, patient 5. High binding cells are admixed with dead cells (*black areas* within regions of bright binding represent dead cells that cannot bind EF5). On H&E counterstaining, pyknotic cells or cellular debris can be seen (data not shown). *C*, patient 6. Regions of very bright binding are seen primarily in keratinized cells. *D*, patient 7. Very little binding is present.

tumor. Immunohistochemical analysis of tumor-infiltrated lymph node sections demonstrated EF5 binding that was similar to that seen in the primary tumor in both patients (Fig. 4; Table 2). Clinically normal tissues (lymph node and endometrium) were studied in patients 1, 6, and 7 (Table 2). In each of these normal tissue samples, fluorescence was <16 (*i.e.*, there was no bright binding). Direct analysis of reference binding rates was not performed in normal tissues. However, assuming similar reference binding values to tumor tissues, this level would represent $<2.5\%$ of maximum.

Nonspecific Antibody Binding and Endogenous Fluorescence. For tissues stained without antibody ("no stain"), binding was negligible with maximum fluorescence values of 3.6–13.8 (Table 2). Tissues stained with competed antibody had similarly low values (8.5–16.6). For sections from *in situ* exposed tissues, there was no relationship between high binding after standard staining *versus* competed staining conditions, suggesting that the inclusion of EF5 with antibody effectively eliminated all specific binding (data not shown).

Eppendorf Measurements. Five of the six patients received Eppendorf measurements, all under general anesthesia (Table 4). Patient 6 did not have needle electrode measurements performed. All patients had at least four tracks recorded (range, 4–7). In three patients, some of these tracks were performed under conditions of high inhaled pO_2. In these patients, the inspired pO_2 was decreased, and additional measurements were taken. Analyses presented in Table 4 include only the lowered pO_2 tracks. There was no correlation between high EF5 binding and low pO_2 values (values <2.5 mm Hg).

DISCUSSION

Until recently, the analysis of hypoxia in tumor tissues has emphasized relatively simple variables, *e.g.*, classification as "hypoxic" *versus* aerobic, hypoxic fraction, median pO_2, percentage of labeled area, and others. However, tissue oxygen content changes gradually with distance from patent vessels (27); therefore, it may be necessary to consider more complex analyses, such as the distribution of pO_2. This is likely to be clinically relevant because theoretical data supports the concept that moderate tumor hypoxia is most important in predicting outcome after fractionated radiation therapy (28). In previous studies of EF5 in experimental tumor systems (25, 29–31), we have emphasized binding as a continual variable. EF5 binding varies continuously through the physiological and pathologically low oxygen ranges found in tumors with a dynamic range (maximum to minimum signal) of approximately two logs (26). We believe that this approach will eventually allow appropriately complex analysis (32). These types of analyses were possible because we have demonstrated that EF5 binding can be quantified using a fluorescent antibody approach. In the current studies, we have measured the maximum (reference) binding of human tumor tissues and compared this with *in situ* binding. Reference binding should optimally be consistent, irrespective of tumor type or site, so that direct comparisons could be made between patients and in the same patient over time. Studies performed on the five SCC tumors studied herein support this observation; the reference binding in the cubes studied varied by a factor of

Table 3 *Histological evaluation of squamous cell cancers*

Patient no.	Site	Differentiation	Keratinization[a]	Host reaction/ lymphs	% necrosis[a]	Stromal reaction[b]	No. of mitosis/ 10 HPF
1	Cervix	Moderate	25%	+1	60	+1	>40
3	Cervix	Moderate–Poor	10%	+2	<10	+2	>80
4	HN[c]	Well–Moderate	70%	+2	10	+2	10
5	HN	Moderate	20%	+2	20	+3	41
6	HN	Well–Moderate	70%	+3	10	+1	<10
7	HN	Moderate–Poor	35%	+2	35	+3	40

[a] % of tissue.
[b] +1, minimal; +2, moderate; +3, severe.
[c] HN, head and neck.

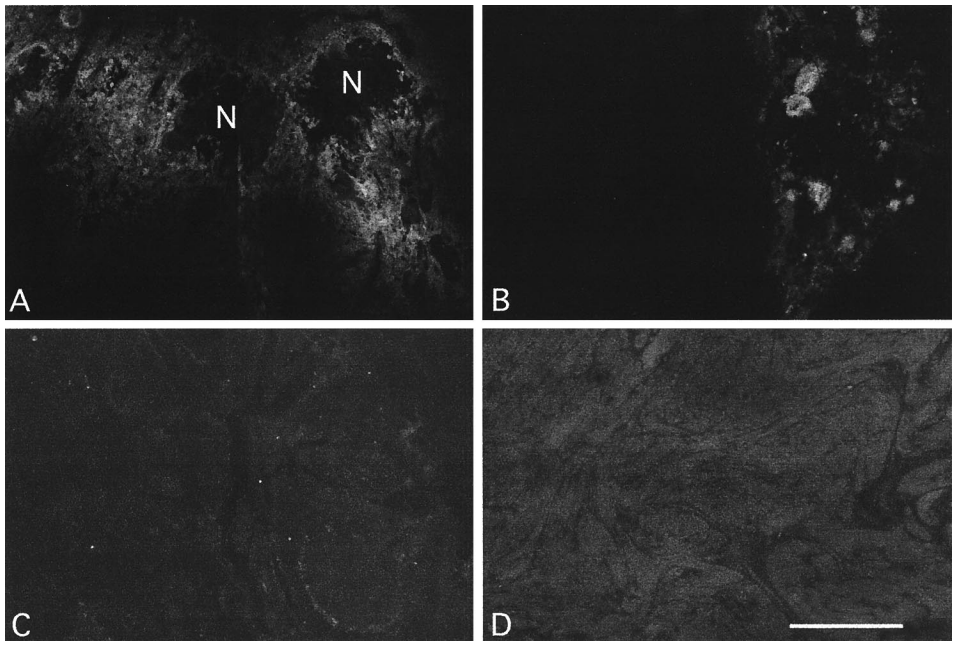

Fig. 4. Photomicrographs of EF5 binding in tumor-infiltrated lymph nodes and normal tissues. Image intensity has been modified to demonstrate distribution of binding. For absolute fluorescence in each section, see Table 2. *Bar*, 500 μm. *A*, binding in tumor-infiltrated lymph node in patient 5. *N*, regions that contained dead/necrotic tissue. During processing, these tissues do not adhere well to the slide and are lost. *B*, binding in tumor-infiltrated lymph node in patient 7. *C*, very little binding is seen in a normal lymph node taken from patient 7 (fluorescence, 13.7). *D*, very little binding is seen in normal endometrium/muscle tissue from patient 1 (fluorescence, 7.8).

<3 (range, 327–905). If further studies support this low variability in reference binding rates between patients, such complex studies would not be required for the future routine evaluation of hypoxia *in situ*. Having demonstrated that the different tumors have a relatively consistent reference rate of binding, we have shown that there is a considerable difference in the maximal binding levels of EF5 observed *in situ*.

Analysis of patterns of binding demonstrate considerable heterogeneity between patient tumors. One of the tumors studied had a corded pattern, and binding was seen along and within the tumor cords (patient 1; Fig. 3). Binding was commonly located adjacent to regions of necrosis; of particular interest is the fortuitous sectioning of a tumor cord perpendicular to its course. At ~200 μm from the blood vessel, regions of viable but hypoxic cells are stained with EF5. At greater cell distances, necrosis was identified (patient 1; Fig. 3). Binding adjacent to macroscopic necrosis was also noted in patient 4. The absolute levels of binding adjacent to the necrosis differed substantially between these two patients; very high binding (86.6% of reference) was seen adjacent to necrosis in patient 4, whereas in patient 1, only minimal levels of binding (14.8% of reference) were present. We interpret these data to suggest that regions of necrosis can occur in areas where only moderate hypoxia occurs, *e.g.*, other nutrients such as glucose may limit cellular viability. In many sections studied, the spatial relationship between blood vessels and regions of binding was similar; blood vessels were at a distance from the regions of binding, characteristic of chronic or diffusion-limited hypoxia. A similarity is noted between the locations of blood vessels and necrosis in Fig. 3 and the observations made by Thomlinson and Gray (27) in H&E-stained histopathological sections of human bronchogenic carcinomas.

The analyses presented herein represent the first quantitative analysis of EF5 binding levels in human tumors. We have compared *in situ* EF5 to *in vitro* EF3 reference binding and demonstrated that *in situ* EF5 binding can be measured and quantified in all tumors. The level of binding, however, as a surrogate for the cellular concentration of oxygen, varies dramatically among tumors. Intratumoral heterogeneity is largest in those patents with regions of very high binding. This observation may account for the lack of correspondence between the Eppendorf needle electrode studies and the EF5 binding values. If the region of highest binding is small, it is possible that the Eppendorf electrode may not traverse these regions. Another consideration is that the needle electrode measurements provide a "snapshot" of hypoxia at the time of surgery, whereas EF5 binding represents a summation of the "history of hypoxia" over the previous 48 h.

In the small number of patients reported herein, there was not a correspondence between percentage of necrosis and the level of EF5 binding. This observation supports the hypothesis that the development of necrosis is multifactorial and not limited to oxygen diffusion. Our cellular studies (26) suggest that maximal EF5 binding *in vitro* occurs in regions of 0.03–0.01% oxygen. Only scattered regions, in about half of the tumors studied herein, approach this level of binding. This is quite different from our observations in transplanted rodent tumors, where maximal EF5 binding is the rule rather than the exception. Binding at a level of ~10-fold less than maximal (work in progress) is much more common in human tumors. On the basis of our

Table 4 *Eppendorf needle electrode values*

Patient no.	FiO_2[a]	Track length (cm)	No. of tracks	No. of measurements/ track	% of values <2.5 mm Hg	% of values <5 mm Hg	% of values <10 mm Hg	median pO_2 (mm Hg)	% reference EF5 binding
1	39%	1.5	4	21	6	8	15	51.5	14.8
3	33%	2.2	4	32	58	64	73	8.8	6.9
4	52%; mask	1.5	4	21	0	26	56	7.5	88.6
5	48%	1.5	3	21	38	67	86	33.5	32.5
6	NA[b]	NA	NA	NA	NA	NA	NA	NA	32.5
7	43%	NA	2	24	63	80	90	3.2	16.5

[a] Via endotracheal tube, unless otherwise noted.
[b] NA, not available.

cellular studies, such levels of binding would be associated with pO_2s of the order of 1% (7.6 mm Hg). This level would be compatible with "intermediate hypoxia" (28). On the basis of a substantially different approach using spheroids, microelectrodes, and tritiated misonidazole (33), it has been suggested that CCI-103F and pimonidazole adducts are not found at cellular pO_2 levels >10 mm Hg (34, 35). We do not know whether this represents a real difference in drug or detection sensitivity because our antibodies can recognize adducts at all physiological oxygen levels.

Because the data presented herein are limited and result from a Phase I trial, statistically valid outcome information is not available. It is of interest, however, that the patients with high N stage or nodal extension from the tumor (patients 4 and 5) had high EF5 binding. High binding was also seen in patient 6. Although this patient did not have nodal disease at the time of analysis, tumor recurrence was documented 7 months after surgery and radiation therapy. In patient 7, moderately high binding was present in the tumor-infiltrated regional lymph node and in the primary tumor. Both patients with low binding uterine cervix cancers have no evidence of disease at 17 and 18 months after surgery.

In the future, we plan to combine analysis of levels of maximal *in situ* binding with determinations of the tissue distribution of binding, on a scale calibrated to cellular pO_2 (36). Whether this will relate to other predictors, such as median pO_2, fraction of labeled area (as used in the pimonidazole trials), tumor fractional hypoxic volume (37), and most importantly, treatment outcome, can only be determined in larger trials. Some of these questions will be addressed in Phase II EF5 studies of patients with head and neck cancer, soft tissue sarcomas, and other sites.

ACKNOWLEDGMENTS

We thank Debbie Smith and Mary Lou Anton for patient nursing care. We also thank several colleagues at the NCI for assistance in the Food and Drug Administration approval process for EF5: Drs. Edward Sauceville, Joe Covey, Ken Snader, Rao Vishnuvajjala, Susan Arbuck, and Percy Ivy.

REFERENCES

1. Kolstad, P. Vascularization, oxygen tension and radiocurability in cancer of the cervix. Universitetsforlaget. Oslo, Norway: Oslo, 1964.
2. Schreiner, P., Siracka, E., Siracky, J., and Manka, I. The effect of anemia on the radiotherapy results of the uterine cervix cancer. Neoplasma (Bratisl.), *22:* 655–660, 1975.
3. Bush, R. S., Jenkins, R. D. T., Allt, W. E. C., Beale, F. A., Bean, H., Dembo, A. J., and Pringle, J. F. Definitive evidence for hypoxic cells influencing cure in cancer therapy. Br. J. Cancer, *37:* 302–306, 1978.
4. Fein, D. A., Lee, W. R., Hanlon, A. L., Ridge, J. A., Langer, C. J., Curran, W. J., Jr., and Coia, L. R. Pretreatment hemoglobin level influences local control and survival of T1–T2 squamous cell carcinomas of the glottic larynx. J. Clin. Oncol., *13:* 2077–2083, 1995.
5. Gatenby, R. A., Kessler, H. B., Rosenblum, J. S., Coia, L. R., Moldofsky, P. J., Hartz, W. H., and Broder, G. J. Oxygen distribution in squamous cell carcinoma metastases and its relationship to outcome of radiation therapy. Int. J. Radiat. Oncol. Biol., Phys., *14:* 831–838, 1988.
6. Hockel, M., Schlenger, K., Aral, B., Mitze, M., Schaffer, U., and Vaupel, P. Association between tumor hypoxia and malignant progression in advanced cancer of the uterine cervix. Cancer Res., *56:* 4509–4515, 1996.
7. Hockel, M., Knoop, C., Schlenger, K., Vorndran, B., Baussmann, E., Mitze, M., Knapstein, P. G., and Vaupel, P. Intratumoral pO_2 predicts survival in advanced cancer of the uterine cervix. Radiother. Oncol., *26:* 45–50, 1993.
8. Brizel, D. M., Sibley, G. S., Prosnitz, L. R., Scher, R. L., and Dewhirst, M. W. Tumor hypoxia adversely affects the prognosis of carcinoma of the head and neck. Int. J. Radiat. Oncol. Biol. Phys., *38:* 285–289, 1997.
9. Nordsmark, M., Overgaard, M., and Overgaard, J. Pretreatment oxygenation predicts radiation response in advanced squamous cell carcinoma of the head and neck. Radiother. Oncol., *41:* 31–39, 1996.
10. Fyles, A. W., Milosevic, M., Wong, R., Kavanagh, M. C., Pintilie, M., Sun, A., Chapman, W., Levin, W., Manchul, L., Keane, T. J., and Hill, R. P. Oxygenation predicts radiation response and survival in patients with cervix cancer. Radiother. Oncol., *48:* 149–156, 1998.
11. Olive, P., Banath, J., and Durand, R. Heterogeneity in radiation-induced DNA damage and repair in tumor and normal cells measured using the "Comet" assay. Radiat. Res., *122:* 86–94, 1990.
12. Raleigh, J. A., Miller, G. G., Franko, A. J., Koch, C. J., Fuciarelli, A. F., and Kelley, D. A. Fluorescence immunohistochemical detection of hypoxic cells in spheroids and tumours. Br. J. Cancer, *56:* 395–400, 1987.
13. Chapman, J. D. The detection and measurement of hypoxic cells in solid tumors. Cancer (Phila.), *54:* 2441–2449, 1984.
14. Evans, S. M., Joiner, B., Jenkins, W. T., Laughlin, K. M., Lord, E. M., and Koch, C. J. Identification of hypoxia in cells and tissues of epigastric 9L rat glioma using EF5 [2-(2-nitro-1*H*-imidazol-1-yl)-*N*-(2,2,3,3,3-pentafluoropropyl)acetamide]. Br. J. Cancer, *72:* 875–882, 1995.
15. Lord, E. M., Harwell, L., and Koch, C. J. Detection of hypoxic cells by monoclonal antibody recognizing 2-nitroimidazole adducts. Cancer Res., *53:* 5271–5276, 1993.
16. Siim, B., Menke, D., Dorie, M., and Brown, J. Tirapazamine-induced cytotoxicity and DNA damage in transplanted tumors: relationship to tumor hypoxia. Cancer Res., *57:* 2922-2928, 1997.
17. Franko, A. J., Koch, C. J., Garrecht, B. M., Sharplin, J., and Hughes, D. Oxygen dependence of binding of misonidazole to rodent and human tumors *in vitro*. Cancer Res., *47:* 5367–5376, 1987.
18. Cline, J. M., Thrall, D. E., Page, R. L., Franko, A. J., and Raleigh, J. A. Immunohistochemical detection of a hypoxia marker in spontaneous canine tumours. Br. J. Cancer, *62:* 925–931, 1990.
19. Hodgkiss, R. J., Jones, G., Long, A., Parrick, J., Smith, K. A., Stratford, M. R. L., and Wilson, G. D. Flow cytometric evaluation of hypoxic cells in solid experimental tumours using fluorescence immunodetection. Br. J. Cancer, *63:* 119–125, 1991.
20. Koh, W. J., Rasey, J. S., Evans, M. L., Grierson, J. R., Lewellen, T. K., Graham, M. M., Krohn, K. A., and Griffin, T. W. Imaging of hypoxia in human tumors with [F-18]fluoromisonidazole. Int. J. Radiat. Oncol. Biol. Phys., *22:* 199–212, 1992.
21. Olive, P. L., and Durand, R. E. Fluorescent nitroheterocycles for identifying hypoxic cells. Cancer Res., *43:* 3276–3280, 1983.
22. Raleigh, J. A., Zeman, E. M., Rathman, M., LaDine, J. K., Cline, J. M., and Thrall, D. E. Development of an ELISA for the detection of 2-nitroimidazole hypoxia markers bound to tumor tissue. Int. J. Radiat. Oncol. Biol. Phys., *22:* 403–405, 1992.
23. Raleigh, J. A., Calkins-Adams, D. P., Rinker, L. H., Ballenger, C. A., Weissler, M. C., Fowler, W. C., Jr., Novotny, D. B., and Varia, M. A. Hypoxia and vascular endothelial growth factor expression in human squamous cell carcinomas using pimonidazole as a hypoxia marker. Cancer Res., *58:* 3765–3768, 1998.
24. Coleman, C. N., Wasserman, T. H., Urtasun, R. C., Halsey, J., Noll, L., Hancock, S., and Phillips, T. L. Final report of the Phase I trial of the hypoxic cell radiosensitizer SR 2508 (etanidazole). Radiation Therapy Oncology Group 83-03. Int. J. Radiat. Oncol. Biol. Phys., *18:* 389–393, 1990.
25. Laughlin, K. M., Evans, S. M., Jenkins, W. T., Tracy, M., Chan, C. Y., Lord, E. M., and Koch, C. J. Biodistribution of the nitroimidazole EF5 (2-[2-nitro-1*H*-imidazol-1-yl]-*N*-(2,2,3,3,3-pentafluoropropyl)acetamide) in mice bearing subcutaneous EMT6 tumors. J. Pharmacol. Exp. Ther., *277:* 1049–1057, 1996.
26. Koch, C. J., Evans, S. M., and Lord, E. M. Oxygen dependence of cellular uptake of EF5 [2-(2-nitro-1*H*-imidazol-1-yl)-*N*-(2,2,3,3,3-pentafluoropropyl)acetamide]: analysis of drug adducts by fluorescent antibodies *versus* bound radioactivity. Br. J. Cancer, *72:* 869–874, 1995.
27. Thomlinson, R. H., and Gray, L. H. The histological structure of some human lung cancers and the possible implications for radiotherapy. Br. J. Cancer, *9:* 539–579, 1955.
28. Wouters, B. G., and Brown, J. M. Cells at intermediate oxygen levels can be more important than the "hypoxic fraction" in determining tumor response to fractionated radiation therapy. Radiat. Res., *147:* 541–550, 1997.
29. Evans, S. M., Jenkins, W. T., Joiner, B., Lord, E. M., and Koch, C. J. 2-Nitroimidazole (EF5) binding predicts radiation resistance in individual 9L s.c. tumors. Cancer Res., *56:* 405–411, 1996.
30. Jenkins, W., Evans, S., and Koch, C. Hypoxia and necrosis in rat 9L glioma and Morris 7777 hepatoma tumors: comparative measurements using EF5 binding and the Eppendorf needle electrode. Int. J. Radiat. Oncol. Biol. Phys., in press, 2000.
31. Lee, J., Fenton, B. M., Koch, C. J., Frelinger, J. G., and Lord, E. M. Interleukin 2 expression by tumor cells alters both the immune response and the tumor microenvironment. Cancer Res., *58:* 1478–1485, 1998.
32. Evans, S. M., Jenkins, W. T., Shapiro, M., and Koch, C. J. Evaluation of the concept of "hypoxic fraction" as a descriptor of tumor oxygenation status. Adv. Exp. Med. Biol., *411:* 215–225, 1997.
33. Gross, M. W., Karbach, U., Groebe, K., Franko, A. J., and Mueller-Klieser, W. Calibration of misonidazole labeling by simultaneous measurement of oxygen tension and labeling density in multicellular spheroids. Int. J. Cancer, *61:* 567–573, 1995.
34. Cline, J. M., Rosner, G. L., Raleigh, J. A., and Thrall, D. E. Quantification of CCI-103F labeling heterogeneity in canine solid tumors. Int. J. Radiat. Oncol. Biol. Phys., *37:* 655–662, 1997.
35. Kennedy, A. S., Raleigh, J. A., Perez, G. M., Calkins, D. P., Thrall, D. E., Novotny, D. B., and Varia, M. A. Proliferation and hypoxia in human squamous cell carcinoma of the cervix: first report of combined immunohistochemical assays. Int. J. Radiat. Oncol. Biol. Phys., *37:* 897–905, 1997.
36. Wilson, D., Laughlin, K., Rozanov, C., Mokashi, A., Vinogradov, S., Lahiri, S., Koch, C., and Evans, S. Tissue oxygen sensing and the carotid body. Adv. Exp. Med. Biol., *454:* 447–454, 1998.
37. Rasey, J. S., Koh, W. J., Evans, M. L., Peterson, L. M., Lewellen, T. K., Graham, M. M., and Krohn, K. A. Quantifying regional hypoxia in human tumors with positron emission tomography of [18F]fluoromisonidazole: a pretherapy study of 37 patients. Int. J. Radiat. Oncol. Biol. Phys., *36:* 417–428, 1996.